Engineering Innovations
ISSN: 2813-1002, Vol. 7, pp 1-6
doi:10.4028/p-sYB7Eh

Submitted: 2023-02-11
Revised: 2023-09-24
Accepted: 2023-09-25
Online: 2023-10-13

Molecular Dynamics Simulation on Shocked Nanocrystalline Aluminum

JU Yuanyuan[a], ZHANG Lei[b*]

Naval Research Institute of PLA, Beijing, China, 100161

[a]juyy2013@163.com, [b]doy2@163.com

Keywords: Molecular Dynamics, Shock Wave, Nanocrystalline Aluminum, Shock Front.

Abstract. The characteristics of shocked nanocrystalline aluminum are investigated by using molecular dynamics method based on the embedded atom method potential function. The result presents the particle velocity profile and the width of shock front in detail. The simulated Hugoniot relations are basically consistent with the experimental data and other molecular dynamics results. The width of shock front decreases with the particle velocity exponentially.

Introduction

The classical molecular dynamics (MD) simulations have been used increasingly to examine the shock compression response of crystalline materials. The massively parallel three-dimensional MD simulations were employed to examine the plasticity induced by shock waves [1-4]. The MD calculations were used to examine the shock wave propagation along [100], [111], and [110] directions in aluminum single crystals [5]. An et al. presented MD simulations of shock-induced plasticity and spall damage in single crystal Ta [6]. The MD method in conjunction with multi-scale shock technique (MSST) is employed to study the melting characteristics of aluminum single crystal under dynamic conditions. [7]. Structural phase transformation in bulk single crystal Cu in different orientation under shock loading of different intensities has been investigated by A. Neogi et al [8]. The evolution of different types of dislocation mechanisms and their mutual interactions during the process of shock loading were investigated by using the MD simulations for Cu [9]. The multimillion atom non-equilibrium MD simulations were used to investigate the effect of crystallographic orientation over the evolution of deformation pathway of single crystal copper under shock compression [10]. The deformation behavior of a single crystal structure and a core-shell Cu@Ni nanoporous (NP) structure under shock loading for a wide range of shock intensities was studied by using MD simulation [11]. The shock compression of a Cu single crystal along the 〈110〉 direction specifically focusing on the mechanisms observed in the elastically compressed and the elastic–plastic transition regions is investigated by using MD simulation [12].

However, most of the previous work involves the single crystal material and only a few of studies involve the nanocrystalline (NC) material compressed by shock wave which results in the elastic-plastic deformation in the compressed region. Recently, NC material has been extensively studied by MD simulations for their numerous beneficial properties. The shock wave propagation in NC was studied by using the MD method and the results showed that the width of the shock wave front increases with grain size, d, as d1/2, and also decreases with the pressure behind the front [13]. The shock-front structures of NC aluminum were investigated in detail by exploring the relationship between the evolution of stress, particle velocity distributions, and the atomistic structures through MD simulations [14]. MD simulations were employed to investigate the deformation mechanisms and microstructure evolution of NC aluminum under compressive deformation at temperatures close to the melting point [15]. The mechanisms of spalling and melting in NC Pb under shock loading were studied by MD simulations. A wide range of shock intensity was considered with the lowest one just above the threshold of solid spallation, while the highest one higher than the threshold of shock melting [16].

In the current letter, the characteristics of shocked NC aluminum are investigated by using MD method based on the EAM potential function. The shock front structure and the Hugonoit relation are obtained. The results provide useful atomistic knowledge on the characteristics of shocked NC aluminum.

Computation Model and Methodology

Potential Function. The potential function plays an important role in the MD simulation, and the embedded-atom-method (EAM) potential is employed in the current study [17]. The functional form of the EAM potentials is given by

$$E_{\text{tot}} = \frac{1}{2}\sum_{i\neq j} V\left(r_{ij}\right) + \sum_{i} F\left(\rho_i\right). \tag{1}$$

$$\rho_i = \sum_{j} \phi\left(r_{ij}\right). \tag{2}$$

where E_{tot} is the total energy, $V(r_{ij})$ the pair potential, and $F(\rho_i)$ the embedding function. $\varphi(r_{ij})$ is the electron density contribution from atom j to atom i. The total electron density ρ_i at an atom position i is calculated via the linear superposition of electron density contributions from neighboring atoms.

Computational Model. The melting behavior of NC aluminum under shock compression is explored using the Large-scale Atomic/Molecular Massively Parallel Simulator (LAMMPS) package [18]. The sample is prepared using the Voronoi construction developed by Chen [19]. The size of the sample is 36 ×18 × 18 nm, totally contains about 70×10^4 atoms. The grain includes about 60×10^4 atoms and the grain boundary includes about 10×10^4 atoms. The configuration of grain is FCC and the crystal direction of the grain is random. The grain boundary is also random. Fig. 1 shows the computation model of NC aluminum. The longest direction is defined as x direction which is along the shock wave direction, and other two directions are defined as y and z direction, respectively. The free boundary conditions are imposed along the shock direction. The periodic boundary conditions (PBC) are imposed to minimize surface and edge effects, simulating a pseudo-infinite lateral dimension in the directions transverse to the shock wave. The system was first minimized using the conjugate gradient method, then thermalized to a temperature of 300K and equilibrated at the temperature using the NVT ensemble, and finally applied various shock waves along the x direction. The time integration step is dt = 0.1 fs, and the total computation time is long enough to ensure the shock wave propagates though the system.

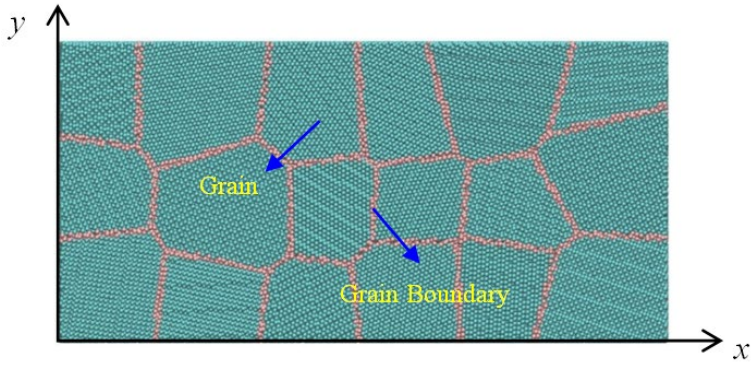

Fig. 1 Computation model of NC aluminum

Results and Discussion

Shock wave profile. Fig. 2 shows the particle velocity profile in the case of u_p=3.6 km/s and the particle velocity distribution at a certain time of t=2 ps. It can be found that a steady shock wave propagates in the NC aluminum and the velocity of the shock wave can be calculated by estimating the distance of the shock wave passing though between two different times. At t=2 ps the particle velocity profile is consistent with the particle velocity distribution with an obvious gradient of velocity. In the compressed region the material is melt while in the uncompressed region the material is still in the initial state.

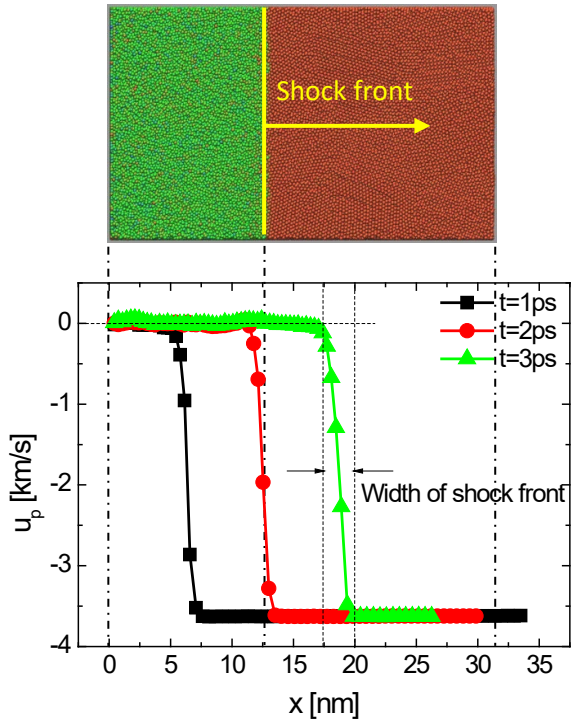

Fig. 2 Velocity profile along the direction of shock wave propagation

Shock Hugoniot Relation. Figure 3 shows the relationship between the shock wave velocity and the particle velocity. The velocity profile is in close agreement with the experimental data [20], showing a linear relationship between up and us given by u_s=5.2284+1.2271u_p. The present results are also basically consistent with the MD results of u_s=5.53292+1.21337u_p obtained by the multi-scale shock technique (MSST) for the aluminum single crystal [7].

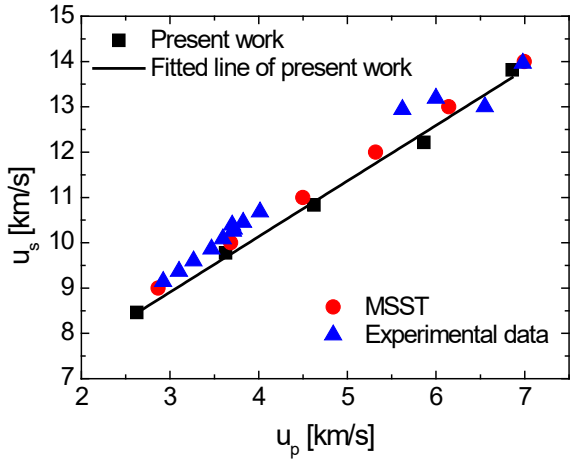

Fig. 3 Relationship between shock wave velocity and particle velocity

The pressure during shock compression for the NC aluminum deviates from the existing experimental values [21, 22] and MD results [23] for aluminum single crystal, as shown in Fig. 4. It can be found that in the high compression region the present results are slightly lower than the experimental values. The same situation occurs in the MD simulations for Ni and Al [24, 25].

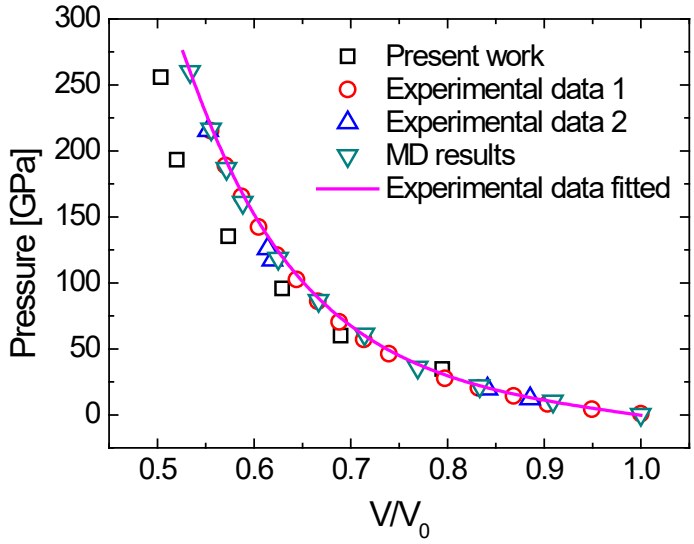

Fig. 4 Relationship between shock pressure and relative volume

In Figure 5 the Hugoniot curve of NC aluminum under different shock pressure is plotted and compared with other results [26, 27]. The present work is nearly the same with the experimental data in the relative low compression region, where the experimental data can be detected. The current work is capable of predicting the temperature in the high compression region, as is difficult for the experimental study.

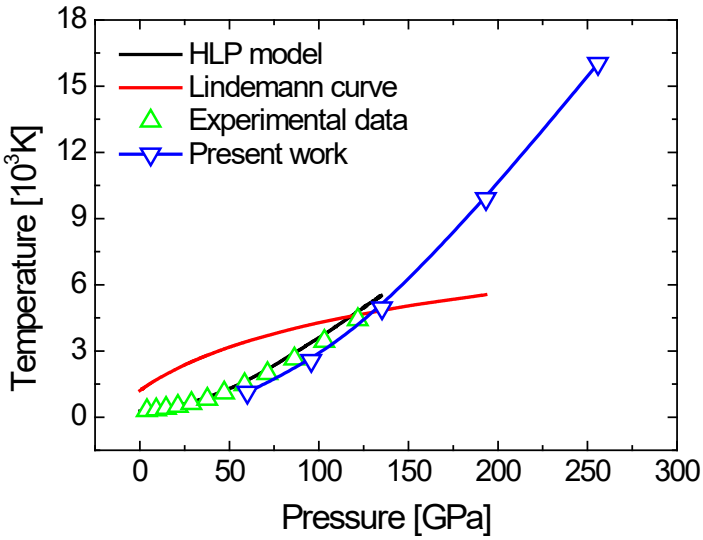

Fig. 5 Dependence of temperature upon shock pressure

Shock Wave Front. Figure 6 shows the relationship between the width of shock front and the particle velocity along the direction of shock wave propagation. The width of the shock front is defined as the profile between the particle velocity u_p=0 and the maximum of the particle velocity, as shown in Fig. 2. It can be seen that the width of shock front λ decreases with the particle velocity u_p. By fitting the simulation results, it is found that the width of shock front decreases with the particle velocity exponentially, given by λ=13.4726×$u_p^{-1.3956}$, as is consistent with the previous work [13].

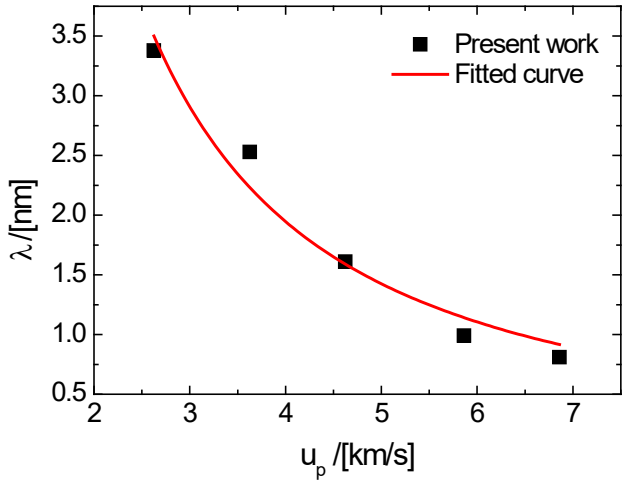

Fig. 6 Relationship between width of shock front and particle velocity

Conclusions

The particle velocity profile, Hugoniot relations, and width of shock front of shocked NC aluminum are obtained by using the MD method. The current study shows that our results are basically consistent with the experimental data and other MD results, and the MD method has the ability of predicting the temperature in the high compression region where it is difficult to study the characteristics of shocked NC aluminum experimentally. The width of shock front decreases with the particle velocity exponentially.

References

[1] Y.Y. Ju, L. Zhang, Molecular Dynamics Simulation of Shock Wave Propagation in Aluminum Single Crystal, Journal of Metastable and Nanocrystalline Materials 36 (2023) 1-6.

[2] I.A. Bryukhanov, Atomistic simulation of the shock wave in copper single crystals with pre-existing dislocation network, International Journal of Plasticity 151 (2022) 103171.

[3] Y. Chen, Z.Y. Jian, S.F Xiao, L. Wang, X.F. Li, K. Wang, H.Q. Deng and W.Y. Hu, Molecular dynamics simulation of shock wave propagation and spall failure in single crystal copper under cylindrical impact, Appl. Phys. Express 14 (2021) 075504.

[4] Y.T. Wang, X.G. Zeng, X. Yang, T.L. Xu, Shock-induced spallation in single-crystalline tantalum at elevated temperatures through molecular dynamics modeling, Computational Materials Science 201 (2022) 110870.

[5] J.A. Zimmerman, J.M. Winey, and Y.M. Gupta, Elastic anisotropy of shocked aluminum single crystals: Use of molecular dynamics simulations, Phys. Rev. B, 83 (2011) 184113.

[6] Q. An, R. Ravelo, T.C. Germann, W.Z. Han, S.N. Luo, D.L. Tonks, and W.A. Goddard, Shock compression and spallation of single crystal tantalum, AIP Conf. Proc., 1426 (2012) 1259-1262.

[7] Y.Y. Ju, Q.M. Zhang, Z.Z. Gong, G.F. Ji, and L. Zhou. Molecular dynamics simulation of shock melting of aluminum single crystal, J. Appl. Phys., 114 (2013) 093507.

[8] A. Neogi, N. Mitra, A metastable phase of shocked bulk single crystal copper: an atomistic simulation study, Sci. Rep. 7, (2017) 7337.

[9] A. Neogi, N. Mitra, Evolution of dislocation mechanisms in single-crystal Cu under shock loading in different directions, Modelling and Simulation in Materials Science and Engineering, 25 (2017) 025013.

[10] A. Neogi, N. Mitra, Shock induced deformation response of single crystal copper: Effect of crystallographic orientation, Computational Materials Science, 135 (2017) 141-151.

[11] A. Neogi; L. He; N. Abdolrahim, Atomistic simulations of shock compression of single crystal and core-shell Cu@Ni nanoporous metals, J. Appl. Phys. 126 (2019) 015901.

[12] A. Bisht, A. Neogi, N. Mitra, G. Jagadeesh, S. Suwas, Investigation of the elastically shock-compressed region and elastic–plastic shock transition in single-crystalline copper to understand the dislocation nucleation mechanism under shock compression. Shock Waves 29 (2019) 913-927.

[13] E.M. Bringa, A. Caro, M. Victoria, and N. Park, The atomistic modeling of wave propagation in nanocrystals, Journal of metals, 57 (2005) 67-70.

[14] W. Ma, W.J. Zhu, and F.Q. Jing, The shock-front structure of nanocrystalline aluminum, Appl. Phys. Lett., 97 (2010) 121903.

[15] A.P. Gerlich, L. Yue, P.F. Mendez, and H. Zhang, Plastic deformation of nanocrystalline aluminum at high temperatures and strain rate, Acta Materialia, 58 (2010) 2176–2185.

[16] M.Z. Xiang, H.B. Hu, and J. Chen, Spalling and melting in nanocrystalline Pb under shock loading: Molecular dynamics studies, J. Appl. Phys., 113 (2013) 144312.

[17] J. Mei, J.W. Davenport, and G.W. Fernando, Analytic embedded-atom potentials for fcc metals: Application to liquid and solid copper, Phys. Rev. B, 43 (1991) 4653.

[18] LAMMPS, Sandia National Laboratories. [online], Available from: http://lammps.sandia.gov.

[19] D. Chen, Structural modeling of nanocrystalline materials, Comput. Mater. Sci., 3 (1995) 327-333.

[20] S.P. Marsh. LASL Shock Hugoniot Data (University of California Press, Berkeley, 1980).

[21] L.V. Al'tshuler, S.B. Kormer, A.A. Bakanova, and R.F. Trunin, The isentropic compressibility of aluminum, copper, lead, and iron at high pressures, Sov. Phys. JETP, 11 (1960) 790.

[22] R.F. Trunin, M. Yu. Belyakova, M.V. Zhernokletov, and Y.N. Sutulov, Izv. Akad. Nauk SSSR, Fiz. Zemli, Shock compression of metal alloys, 2 (1991) 99.

[23] D.K. Belashchenkoa, A.V. Vorotyagina, and B.R. Gelchinsky, Computer simulation of aluminum in the high-pressure range, High Temperature, 49 (2011) 656.

[24] L. Koči, E.M. Bringa, D.S. Ivanov, J. Hawreliak, J. McNaney, A. Higginbotham, L.V. Zhigilei, A.B. Belonoshko, B.A. Remington, and R. Ahuja, Simulation of shock-induced melting of Ni using molecular dynamics coupled to a two-temperature model, Phys. Rev. B, 74 (2006) 012101.

[25] A. Kubota, D.B. Reisman, and W.G. Wolfer, Dynamic strength of metals in shock deformation, Appl. Phys. Lett., 88 (2006) 241924.

[26] J.A. Moriarty, D.A. Young, and M. Ross, Theoretical study of the aluminum melting curve to very high pressure, Phys. Rev. B, 30 (1984) 578.

[27] R.F. Trunin. The properties of condensed matter under high pressure and high temperature Translated by J. W. Han (Institute of Fluid Physics, CAEP, Mianyang, 1996) pp.40-52. (in Chinese)